

Karhunen-Loève transform applied to region-based segmentation of color aerial images

J. C. Devaux

P. Gouton

F. Truchetet, MEMBER SPIE

Le2i—Université de Bourgogne

BP47870

21078 Dijon Cedex, France

E-mail: f.truchetet@iutlecreusot.u-bourgogne.f

Abstract. The use of the Karhunen-Loève transform (KLT) for region-based segmentation of aerial images by color and textural attributes is presented. Our aerial images are shown to be homogeneous color images within the Karhunen-Loève color representation space, which means they can be represented more easily and the region-based segmentation algorithms can be optimized. For texture analysis, the KLT is the basis of the local linear transform (LLT) and allows structural information about textures to be represented in an optimal and condensed manner. The LLT provides a system of textural analysis in the form of an adapted filter bank. We end the paper by presenting a method for merging texture and color segmentations. © 2001 Society of Photo-Optical Instrumentation Engineers. [DOI: 10.1117/1.1385166]

Subject terms: image processing; aerial color images; Karhunen-Loève transform; region-based segmentation; textural analysis; local linear transform; cooperative segmentation.

Paper 200026 received Jan. 20, 2000; revised manuscript received Dec. 1, 2000; accepted for publication Jan. 29, 2001.

1 Introduction

This paper addresses the problem of region-based segmentation of color aerial images for the purpose of mapping the plant cover of the area overflowed. Region-based segmentation of images consists in dividing up the image topologically with each region distinguished by attributes.¹ This subject is dealt with extensively in the literature with regard to both the type of attributes (intensity, texture, etc.) and the methods used.²

As a result of the increasing use of color for image processing, many researchers have investigated the question of extending the techniques used for black-and-white images to the three-dimensionality of color images.³ Carron suggested an interesting approach based on merging color components in HSI space to yield a one-dimensional, composite image that could readily be exploited by conventional techniques.⁴ Unfortunately, this method is ill suited to automatic segmentation, since the choice of parameters remains empirical.

To overcome this problem we present here a region-based segmentation method directly adapted to images, whether for color attributes or for textural attributes. Because of the noncorrelation of the data, we use the Karhunen-Loève transform (KLT).

The KLT was long considered to be too complex to use, as a large storage capacity and long computing time are required to estimate the covariance matrix.⁵ However, developments in computing and the introduction of effective approximation methods (DCT, DEST, etc.),⁶ have made the KLT a widely used statistical technique.

The KLT brings out the linear connections between the variables x_i of any measurement vector X .⁷ It is a factorial method in that the number of variables is not reduced by selecting just some of them, but by constructing new syn-

thetic variables by linear combination of the initial variables.

The KLT therefore results in a better representation of data in the sense of the least-squares criterion. It is optimal in that it is a canonical transformation minimizing the mean squared error between the truncated representation and the actual data.⁸ Furthermore, it ensures perfect decorrelation of variables. For all these reasons the KLT has become an important tool in a wide range of fields and applications. Tan and Kittler thoroughly reviewed the use of the KLT for color texture.⁹

In Sec. 2 we summarize the main properties of the KLT. This transform is applied to aerial images, and some simplifications are deduced from its properties. Thus, a region-based segmentation algorithm based on a color criterion can be applied.

Then we apply the KLT to textural analysis by introducing the local linear transform (LLT), which is a textural analysis method using a bank of filters adapted to the image. A supervised classification algorithm for segmenting the textures of our images is proposed.

In Sec. 4, a cooperative segmentation method for supervising color segmentation by texture segmentation is proposed. Finally, the most relevant region-based segmentation for our color aerial images is given.

2 Segmentation in Karhunen-Loève Space

2.1 Karhunen-Loève Transform

A color image is represented naturally on the basis of a three-dimensional coordinate system. The KLT enables us to find new representational axes where the energy contained on each axis is optimally distributed. Total energy is preserved in this transformation. But all reference to the human visual system is lost in the process.



Fig. 1 Color aerial image.

Applied to color images, the KLT is defined by $K = A(I - m_I)$, where I is the initial image vector [$I = (I_R, I_G, I_B)^T$], m_I is the mean vector of the image [$m_I = (m_R, m_G, m_B)^T$] and A is the transformation matrix formed by the eigenvectors of the image covariance matrix

$$C_{RGB} = \begin{bmatrix} C_{RR} & C_{RG} & C_{RB} \\ C_{GR} & C_{GG} & C_{GB} \\ C_{BR} & C_{BG} & C_{BB} \end{bmatrix}$$

with $C_{ks} = (1/N) \sum_{i=0}^{N-1} [I_k(i) - m_{I_k}] [I_s(i) - m_{I_s}]^T$, where $k, s = R, G, B$, and N is the number of pixels in the image. We have

$$A = \begin{bmatrix} k_{11} & k_{12} & k_{13} \\ k_{21} & k_{22} & k_{23} \\ k_{31} & k_{32} & k_{33} \end{bmatrix},$$

where $\mathbf{k}_1 = (k_{11}, k_{12}, k_{13})^T$, $\mathbf{k}_2 = (k_{21}, k_{22}, k_{23})^T$, and $\mathbf{k}_3 = (k_{31}, k_{32}, k_{33})^T$ are the eigenvectors of C_{RGB} and therefore the axes of the transform space K .¹⁰

The energy contained on the new axes is distributed decreasingly in the importance of the axis: $\lambda_1 > \lambda_2 > \lambda_3$, where λ_1 , λ_2 , and λ_3 are the eigenvalues of the covariance matrix C_{RGB} associated respectively with the eigenvectors \mathbf{k}_1 , \mathbf{k}_2 , and \mathbf{k}_3 . The KLT applied to a color aerial image (Fig. 1) breaks up as in Fig. 2. It can clearly be seen that the energy contained on the new axes is distributed decreasingly in the importance of the axis. Consequently the KLT allows us to determine the statistical properties of the color

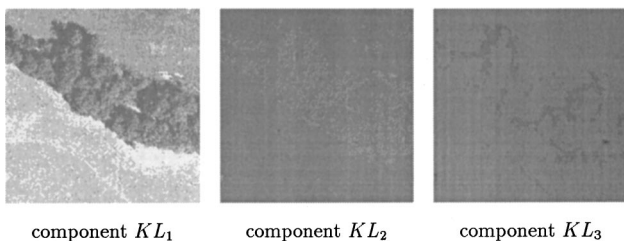


Fig. 2 Projection of color image in KL space.

space, i.e., each color scene has a specific distribution of light energy that can be represented in a system of chromatic coordinates.

2.2 Homogeneous Color Image

The first important property of the KLT is the total noncorrelation of the transform data.^{10,11} A fundamental corollary for image processing derives from this property: transform images can be processed separately and independently. In addition, for color images, studies show that it is useful to separate out the components for colorimetric analysis: luminance information is contained on the KL_1 axis, and chrominance information on the KL_2 and KL_3 axes.^{7,8,12}

The second important property of the KLT is that it is optimal in that it leads to the greatest possible difference in variance distributions on the axes. Accordingly the overall signal energy is preserved.⁶ In KL space, the total energy contained in the transformed image is defined by the relation

$$\text{Energy}(K) = \lambda_1 + \lambda_2 + \lambda_3 = 100\%.$$

Therefore, in KL space, all the energy of the image is stored in the sum of the eigenvalues. Moreover, the energy of each component is given by its eigenvalue. As by definition $\lambda_1 > \lambda_2 > \lambda_3$, the KL_1 axis is energetically preponderant over KL_2 , which in turn has more energy than KL_3 .

We therefore studied the energy of each axis for a series of 12 aerial test images of which Fig. 1 is an example. The contribution of each axis to the total energy is defined as a percentage by

$$E_{KL_k} = \frac{\lambda_k}{\lambda_1 + \lambda_2 + \lambda_3}, \quad \text{where } k = 1 \text{ or } 2 \text{ or } 3.$$

On average, $E_{KL_1} = 98.4\%$, $E_{KL_2} = 1.1\%$ and $E_{KL_3} = 0.5\%$. The results clearly show the importance of the KL_1 axis compared with the other two.

We will now therefore define an energy criterion for determining the relevance of the information on KL_3 . To do this, an image representation quality coefficient Q is defined for measuring the quantity of energy preserved when the KL_3 axis is deleted:

$$Q = \frac{\lambda_1 + \lambda_2}{\lambda_1 + \lambda_2 + \lambda_3}.$$

The closer Q is to 100%, the better the approximation of the image by the two basis vectors \mathbf{k}_1 and \mathbf{k}_2 .

The coefficient Q has been calculated for our set of images. In all cases, Q is greater than 98.5%. As an image is segmented on the basis of an energy criterion, the KL_3 axis can be deleted without significant loss of relevant information, which is tantamount to projecting the data on the plane (KL_1, KL_2). Therefore the KL_1 axis contains the luminance information and the KL_2 axis alone contains the color information: we have a homogeneous color image.

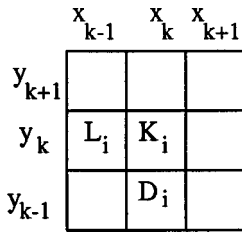


Fig. 3 Mask for color segmentation.

2.3 Region-Based Segmentation

Therefore the KL_1 and KL_2 components will be separately segmented, and the resulting segmentations will be merged.

A classification algorithm is chosen for the segmentation procedure.¹³ This algorithm comprises two parts:

1. *Multiple thresholding:* As the histograms of our aerial images do not include any well-defined modes, we have decided arbitrarily to divide up the gray scale into n classes of equal size.
2. *Labeling of connex components:* To recover the regions of the image, a connex-component-labeling algorithm is applied to the thresholded image.

The same number of modes for multithresholding are used on the two components. Both segmentations are merged as per the mask in Fig. 3 as follows:

- If $K_1 = D_1$ and $K_2 = D_2$ and $K_1 \neq L_1$ and $L_2 \neq L_2$ then $Reg(K) = Reg(D)$.
- If $K_1 \neq D_1$ and $K_2 \neq D_2$ and $K_1 = L_1$ and $K_2 = L_2$ then $Reg(K) = Reg(L)$.
- If $K_1 = D_1$ and $K_2 = D_2$ and $K_1 = L_1$ and $K_2 = L_2$ then $Reg(K) = Reg(D) = Reg(L)$.
- In all other cases $Reg(K)$ is created.

This method is now applied to a test image (Fig. 1). The resulting segmentation is shown in Fig. 4 after eliminating the small regions of less than 10 pixels by merging them with the adjacent region of the nearest color. We obtain 322 regions for $n = 5$.

The psychovisual results seem to be correct: the main regions of the images are clearly detected. However, our

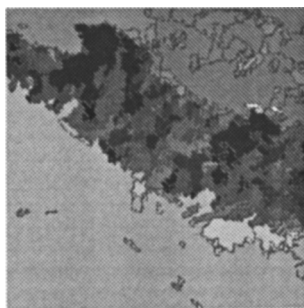


Fig. 4 Color segmentation in KL space.

results show a tendency to oversegmentation, particularly in textured regions. To overcome this problem, LLT texture analysis is now introduced.

3 LLT Texture Analysis

Texture is one of the most important attributes for image segmentation. The human visual system performs extremely well texture analysis, since the notion is intuitively linked to the homogeneous appearance of a surface, i.e., spatial information relative to the surface condition of the area under consideration.

However, image segmentation by texture analysis is one of the most difficult issues in image processing, as there is no universally accepted definition of texture but only an essential property: texture is translation-invariant (it leaves the same impression on the visual system whichever part of texture is observed).

Gagalowicz defined two types of texture:¹⁴

- *Macrottextures:* They correspond to a structural, deterministic approach. The arrangement of primitives is the point of interest.
- *Microtextures:* They correspond to a probabilistic approach. A particular primitive is the point of interest.

In his synthesis of texture analysis methods, Haralick¹⁵ also presents this duality in terms of structural methods (corresponding to the macroscopic approach) and statistical methods (corresponding to the microscopic approach). The second approach fits our type of image more closely. In this context, we develop here a recent statistical approach: the filter-bank approach, and more particularly the local linear transform (LLT).

3.1 DCT Color Space

The KLT is optimal for each image; the eigenvalues and eigenvectors for each color image to be decomposed in this base must therefore be calculated, notably increasing the calculation time. In addition, for some applications, a fixed decomposition basis is required to be able to compare color images. This is the case with texture analysis, where we must compare attributes from different color images.

To overcome these constraints, effective approximation methods to the KLT have been implemented, such as the discrete cosine transform (DCT), which is one of the closest approximations to the KLT.⁶

The transition matrix from *RGB* to DCT is given by the following canonical form:

$$W_m(k) = \begin{cases} \sqrt{\frac{1}{\sqrt{3}}} & \text{for } m=1 \text{ and } k=1,2,3, \\ \sqrt{\frac{2}{3}} \cos[(2k-1)(m-1)\pi/6] & \text{for } m=2,3 \text{ and } k=1,2,3. \end{cases}$$

This space preserves the main characteristics of KL space, i.e., the noncorrelation of data and preservation of total energy.¹⁰ So, in this paper, the DCT is just used to obtain the color components.

x_1	x_2	x_3
x_4	x_5	x_6
x_7	x_8	x_9

Fig. 5 3×3 neighborhood for LLT.

3.2 The Local Linear Transform

3.2.1 Introduction

In 1980 Laws introduced two-dimensional linear filtering techniques for texture analysis.¹⁶ He defined a finite-pulse-response filter bank. Each filter extracts from the image a particular structural component of texture, oriented in the direction of the gradient favored by the filter. To improve the method, Ade proposed a filter bank adapted to the image by basing it on the eigenvectors of the image.¹⁷ The LLT was born. Unser formalized this concept of texture analysis by adapted linear filtering.¹⁸

We propose to extend this method for analyzing color texture by extracting both spatial (i.e., texture) and spectral (i.e., color) attributes from a color image.

3.2.2 Definition

Texture is characterized by the pixel neighborhood properties; therefore, an observation window for studying the statistical properties of texture in a given neighborhood of a pixel of the image must be defined. Provent¹⁹ proposes several types of neighborhood. We use a 3×3 neighborhood to minimize calculation, and center it on pixel x_5 (Fig. 5) to cover the most isotropic neighborhood possible.

Let X be the measurement column vector defining the neighborhood [$X = (x_1, \dots, x_9)^T$]; X is termed the local neighborhood vector (LNV). If the image is described by a statistical model, each variable x_i is considered to be random; a particular texture will be characterized by the different statistics associated with the LNV.¹⁹ These statistics are calculated from all of the M realizations of the vector X determined by mask scanning of the neighborhood on the image.

To decorrelate information, the KLT is now applied to the LNV vector X . To do this, the covariance matrix C_X of X is constructed:

$$C_X = \begin{bmatrix} E(x_1^2) & \dots & E(x_9, x_1) \\ \vdots & \ddots & \vdots \\ E(x_1, x_9) & \dots & E(x_9^2) \end{bmatrix},$$

where E is the centered intercorrelation ($E(x_i, x_j) = (1/M) \sum_{k=0}^{M-1} [(x_i^k - \mu(x_i))(x_j^k - \mu(x_j))]^T$). The matrix C_X has dimension 9×9 . By diagonalizing it, nine eigenvalues in decreasing rank order ($\lambda_1 > \lambda_2 > \dots > \lambda_9$) and nine eigenvectors Φ_n corresponding to those eigenvalues are obtained.

The filter bank adapted to the image by associating the corresponding linear filter $\Phi_n(i, j)$ with each eigenvector Φ_n can be defined:

$$\begin{aligned} \Phi_n &= (\phi_{n1}, \phi_{n2}, \dots, \phi_{n9})^T \Leftrightarrow \Phi_n(i, j) \\ &= \begin{bmatrix} \phi_{n1} & \phi_{n2} & \phi_{n3} \\ \phi_{n4} & \phi_{n5} & \phi_{n6} \\ \phi_{n7} & \phi_{n8} & \phi_{n9} \end{bmatrix}. \end{aligned}$$

The LLT of the image is then defined by

$$Y_n(i, j) = X \Phi_n(i, j).$$

The LLT is consequently the projection of the image onto its filter bank. Y_n is termed the *channel image*.

3.2.3 Properties

An essential property of the LLT is the conservation of the image's total energy: the energy after filtering is distributed over the different channels. Each channel represents a particular direction of the texture (diagonal, horizontal, vertical, etc.), and the channels with high indices contain little textural information: their contribution to the total energy is insignificant. Moreover, by calculating the local variance σ_n^2 on an $A \times B$ window of channel n ,

$$\sigma_n^2(i, j) = \frac{1}{AB} \sum_{a=-A/2}^{A/2} \sum_{b=-B/2}^{B/2} [y_n(i+a, j+b) - \bar{y}_n]^2,$$

Provent et al.²⁰ showed that the distribution of σ_n is centered on the eigenvalue λ_n of channel n .

This essential property allows us to use the LLT to analyze texture. Consider two textures T_1 and T_2 and the filter bank adapted to each texture. We will represent the two textures on the filter bank adapted to T_1 . The local variances in the T_1 channels will be centered on the eigenvalues of T_1 , whereas the local variances in T_2 channels will be centered on arbitrary values.

Moreover, the study of variance distributions shows histograms with a shape that can be approximated by a Gaussian-type normal law.²⁰ We can deduce from this that the domains in attribute space are unimodal, allowing us to simplify our texture analysis algorithm.

3.3 Texture Analysis

Since attribute classes are unimodal, a supervised classification algorithm based on Euclidean distance can be used to analyze texture.¹⁹ Supervised classification consists in determining the division of attribute space that best discriminates between classes, according to a chosen criterion. This method requires *a priori* knowledge of the number of classes of the image and of the representatives of these classes. As with most supervised methods, our algorithm consists of two stages.

3.3.1 The learning stage

For representative samples of textures in the image, the characteristic attributes of each sample (center of gravity of

the class) are determined on a 32×32 pixel window at the center of the sample. Consequently, the statistical analysis is conducted on 900 realizations of the LNV (32×32 edges), representing a characteristic statistical population.

For an image to be segmented with p different textures, a representative vector $A^q = (a_1^q, a_2^q, \dots, a_n^q)$, where n is the number of attributes and q varies from 1 to p , is obtained for each texture.

3.3.2 The recognition stage

The image is scanned through a 16×16 analysis window, because the texture must be homogeneous inside. The choice of analysis window remains empirical, but a 16×16 window contains the whole textural information for our aerial color images. For each pixel the attribute vector (here the local variance) $Z^q = (z_1^q, z_2^q, \dots, z_n^q)$ is determined over this window. The Euclidean distance D^q between the vector Z and the vector A for class q is then calculated:

$$D^q = \left[\sum_{i=1}^n (z_i^q - a_i^q)^2 \right]^{1/2}.$$

But with Euclidean distance some attributes (those with the greatest weights) tend to dominate the measurement. This difficulty can be overcome by using other distances (such as the Mahalanobis distance¹⁹). In our case, we choose to normalize the parameters so they are of equal weight. The normalized Euclidean distance D_N^q between the vector Z and the vector A for class q is computed:

$$D_N^q = \left[\sum_{i=1}^n \frac{(z_i^q - a_i^q)^2}{(a_i^q)^2} \right]^{1/2}.$$

A *distance image* is therefore obtained for each class q of the initial image: the pixel to be classified belongs to the texture class minimizing distance D_N^q .

To analyze a color image the LLT must be applied to the three color components. We consequently have 3×9 eigenvalues and therefore 27 texture attributes with which to characterize the image, which is a large number. Since only the first channels, and therefore the first eigenvalues, have significant energy levels, we take as texture attributes the first three eigenvalues of each component. These represent 90% to 95% of texture energy on the component for our aerial images, a sufficient quantity to discriminate textures. Our classifier is therefore fed by nine attributes.

3.3.3 Results

The algorithm is applied to the test image (Fig. 1) composed of three different textures. Figure 6 shows the result obtained. It is very conclusive: the large regions are perfectly defined. However, the size of the analysis window means the region boundaries are poorly located.

The LLT therefore leads to an optimal solution for supervised segmentation of texture images. It is based on the fact that the mean energy of a texture is conserved by filtering and is distributed around eigenvalues of its adapted transformation. Moreover, this method solves the difficult problem of the choice of the most relevant texture attributes.

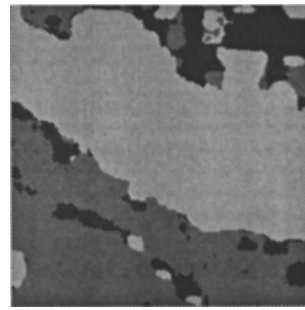


Fig. 6 Texture analysis by LLT.

The problem of the analysis-window size is critical, and it would be interesting to adapt its size locally to the textural homogeneity. As a result, the region boundaries would be better located.

4 Color-Texture Merger

For a color image and using the two algorithms presented previously, two types of complementary segmentation are obtained:

- Color segmentation, which is oversegmented and with well-localized region boundaries (Fig. 4).
- Texture segmentation, which is undersegmented with poorly localized boundaries between textures (Fig. 6).

Superimposition of the region's color outline onto the texture image shows two types of color regions (Fig. 7): color regions that are homogeneous in texture and those that are not.

Our color and texture segmentation merger algorithm will include two stages (Fig. 8). The first stage consists in making each color region homogeneous in texture. To do that, we ascribe to each color region the texture with the largest area (in pixels) in that region. Figure 9 shows the result: each color region now has a homogeneous texture. This first stage improves the localization of boundaries between textures.

The second stage of our algorithm allows adjacent regions with the same texture and similar color components (in our case a difference of 20 gray-scale levels in R , G , and B) to be merged. The characteristic attributes of the regions (size, color, etc.) are modified when merged. Figure 10 shows the result of the color-texture merger algorithm.

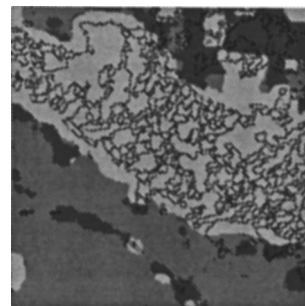


Fig. 7 Superimposition of the region's color outline onto the texture image.

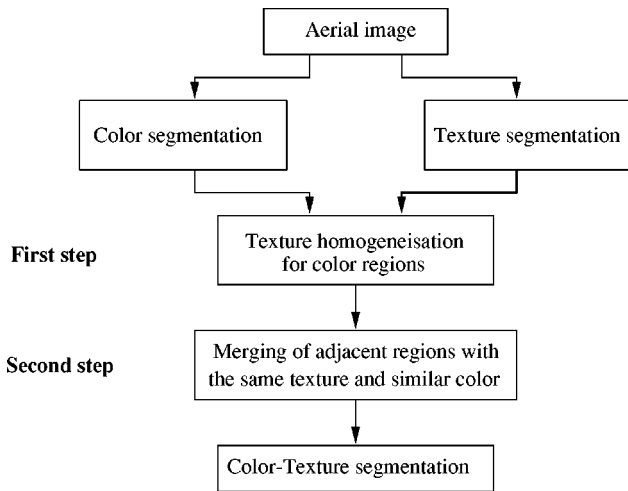


Fig. 8 Color-texture merger algorithm.

Oversegmentation of the textured zones is greatly reduced. The number of regions in the image is now 120. Consequently, our method of texture-supervised color segmentation greatly improves the result obtained, which is much closer to the actual situation on the ground as provided by the ecology specialist.

5 Conclusions

We have presented a number of applications of the Karhunen-Loève transform for color image analysis. The KLT is based on knowledge of the statistical properties of color space, i.e., each color scene has a specific distribution of light energy which can be represented by a system of chromatic coordinates.

We have thus been able to define homogeneous color images, allowing us to simplify their representation. We adapted a region-based segmentation algorithm to process color images represented in KL space.

To improve color aerial image segmentation, we applied the KLT to texture analysis using the local linear transform. The texture segmentation obtained is used to supervise color segmentation and so limit oversegmentation. Our algorithm thus produces relevant results on color aerial images. Comparison with the situation on the ground largely validates these results for the application in question.

However, our algorithm still displays a few limitations on a number of very highly textured images. To overcome these defects we might, for example, give a degree of con-

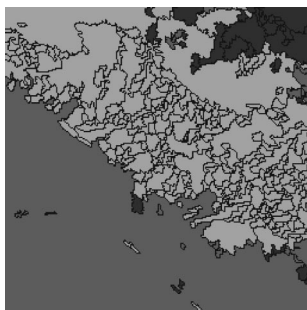


Fig. 9 Texture homogenization for color regions.

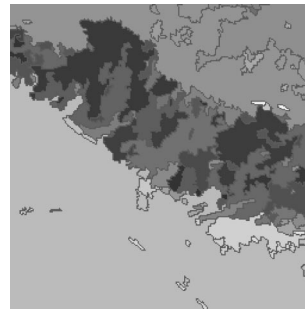


Fig. 10 Result of the color-texture merger.

fidence to the texture segmentation obtained, depending on the distance calculated during the classification stage. Greater or lesser allowance would then be made for the texture, depending on its degree of relevance. It may also be interesting to look at cooperative approaches for further improvements.

Acknowledgments

This work was supported by the Council of Europe and the Conseil Régional de Bourgogne.

References

1. S. W. Zucker, "Region growing: childhood and adolescence," *Comput. Graph. Image Process.* **5**, 382–399 (1976).
2. R. M. Haralick and L. G. Shapiro, "Survey, image segmentation techniques," *Comput. Vis. Graph. Image Process.* **29**, 100–132 (1985).
3. Y. I. Ohta, T. Kanade, and T. Sakai, "Color information for region segmentation," *Comput. Vis. Graph. Image Process.* **13**, 222–241 (1980).
4. T. Carron, "Segmentations d'images couleur dans la base teinte-luminance-saturation: approche numérique et symbolique," PhD Thesis, Univ. de Savoie, France (1995).
5. A. Levy and M. Lindenbaum, "Sequential Karhunen-Loève basis extraction and its application to images," in *IEEE International Conf. on Image Processing*, Vol. 2, pp. 456–460, Chicago (1998).
6. M. Unser, "On the approximation of the discrete Karhunen-Loève transform for stationary processes," *Signal Process.* **7**(3), 231–249 (1984).
7. A. Brun Buisson, V. Lattuati, and D. Lemoine, "Présegmentation d'images couleur par la transformée de Karhunen-Loève," in *14^{ème} Colloque GRETSI*, pp. 743–746, Juan les Pins, France (1993).
8. J. H. Lee, B. H. Chang, and S. D. Kim, "Comparison of colour transformation for image segmentation," *Electron. Lett.* **30**(20), 1660–1661 (1994).
9. T. S. C. Tan and J. Kittler, "Colour texture analysis using colour histogram," *IEE Proc. Vision Image Signal Process.* **141**(6), 403–412 (1994).
10. R. K. Kouassi, J. C. Devaux, P. Gouton, and M. Paindavoine, "Application of the Karhunen-Loève transform for natural color images analysis," in *31st Asilomar Conf. on Signals, Systems and Computers Proc.*, Vol. 2, pp. 1740–1744, IEEE Computer Society, Pacific Grove, CA (1997).
11. N. Tsapatsoulis, V. Alexopoulos, and S. Kollias, "A vector based approximation of KLT and its application to face recognition," in *Signal Processing IX*, Vol. 3, pp. 1581–1584, Rhodes, Greece (1998).
12. I. A. O. Luna, "Analyse en composantes principales d'une image couleur," PhD Thesis, Inst. National Polytechnique de Grenoble, France (1985).
13. J. Devaux, R. Kouassi, P. Gouton, and F. Truchetet, "Region-based segmentation of color images: application to aerial image cartography," in *31st Asilomar Conf. on Signals, Systems and Computers Proc.*, Vol. 2, pp. 1735–1739, IEEE Computer Society, Pacific Grove, CA (1997).
14. A. Gagalowicz, "Vers un modèle de textures," PhD Thesis, Univ. Pierre et Marie Curie, Paris VI (1983).
15. R. M. Haralick, "Statistical and structural approaches to texture," *Proc. IEEE* **67**(5), 786–804 (1979).
16. K. L. Laws, "Texture image segmentation," PhD Thesis, Image Processing Inst., Univ. of Southern California (1980).

17. F. Ade, "Characterization of textures by eigenfilters," *Signal Process.* **5**, 451–457 (1983).
18. M. Unser, "Local linear transforms for texture measurements," *Signal Process.* **11**, 61–79 (1986).
19. P. Provent, "Segmentation d'images par analyse statistique de textures: application aux images échocardiographiques," PhD Thesis, Univ. de Paris XII, Val de Marne, France (1991).
20. P. Provent, J. Lemoine, and E. Petit, "Segmentation optimale d'images de texture par transformations adaptées multiples," *Traitement du Signal* **11**(1), 43–56 (1994).

Jean-Christophe Devaux received his PhD in image processing from the Université de Bourgogne, France, in 2000. He is currently assistant professor at the Université Louis Pasteur, Strasbourg, France. His research interests include image processing, color images, multiresolution segmentation, and pattern recognition.

Pierre Gouton obtained a PhD in components, signals and systems at the University of Montpellier 2 (France) in 1991. From 1988 to 1992, at the Laboratory of Electric Machine of Montpellier, he worked on passive power components. Since 1993, as an assistant professor at the Université de Bourgogne, France, he has integrated

the image processing group at Le2i, the laboratory of electronic, computer and imaging sciences at the same university. His main topic of research is the segmentation of images by both linear methods (edge detectors) and nonlinear methods (mathematical morphology, classification). He is a member of ISIS (a research group in signal and image processing of the French National Scientific Research Committee) and also a member of the French Color Group. Since December 2000, he has been a member of the Research Directorate Authority (HDR).

Fred Truchetet received a master's degree in physics at Dijon University, France, in 1973, and a PhD in electronics at the same university in 1977. For two years he was with Thomson-CSF as a research engineer, and he is currently a full professor and the head of the image-processing group at Le2i, the laboratory of electronic, computer, and imaging sciences, at the Université de Bourgogne, France. His research interests are focused on image processing for artificial vision and inspection, and particularly on wavelet transforms, multiresolution edge detection, and image compression. He is a member of SPIE, IEEE, and ISIS (a research group of the CNRS).